Behavioral/Systems/Cognitive

Neurogranin/RC3 Enhances Long-Term Potentiation and Learning by Promoting Calcium-Mediated Signaling

Kuo-Ping Huang,[1]* Freesia L. Huang,[1]* Tino Jäger,[2] Junfa Li,[1] Klaus G. Reymann,[2] and Detlef Balschun[2]

[1]Section on Metabolic Regulation, Endocrinology and Reproduction Research Branch, National Institute of Child Health and Human Development, National Institutes of Health, Bethesda, Maryland 20892-4510, and [2]Leibniz Institute for Neurobiology, D-39008 Magdeburg, Germany

In neurons, neurogranin (Ng) binds calmodulin (CaM), and its binding affinity is reduced by increasing Ca^{2+}, phosphorylation by PKC, or oxidation by oxidants. Ng concentration in the hippocampus of adult mice varied broadly ($Ng^{+/+}$, ~160–370 and $Ng^{+/-}$, ~70–230 pmol/mg); the level in $Ng^{+/+}$ mice is one of the highest among all neuronal CaM-binding proteins. Among $Ng^{+/-}$ mice, but less apparent in $Ng^{+/+}$, a significant relationship existed between their hippocampal levels of Ng and performances in the Morris water maze. $Ng^{-/-}$ mice performed poorly in this task; they also displayed deficits in high-frequency-induced long-term potentiation (LTP) in area CA1 of hippocampal slices, whereas low-frequency-induced long-term depression was enhanced. Thus, compared with $Ng^{+/+}$ mice, the frequency–response curve of $Ng^{-/-}$ shifted to the right. Paired-pulse facilitation and synaptic fatigue during prolonged stimulation at 10 Hz (900 pulses) were unchanged in $Ng^{-/-}$ slices, indicating their normal presynaptic function. Measurements of Ca^{2+} transients in CA1 pyramidal neurons after weak and strong tetanic stimulations (100 Hz, 400 and 1000 msec, respectively) revealed a significantly greater intracellular Ca^{2+} ($[Ca^{2+}]_i$) response in $Ng^{+/+}$ compared with $Ng^{-/-}$ mice, but the decay time constants did not differ. The diminished Ca^{2+} dynamics in $Ng^{-/-}$ mice are a likely cause of their decreased propensity to undergo LTP. Thus, Ng may promote a high $[Ca^{2+}]_i$ by a "mass-action" mechanism; namely, the higher the Ng concentration, the more Ng–CaM complexes will be formed, which effectively raises $[Ca^{2+}]_i$ at any given Ca^{2+} influx. This mechanism provides potent signal amplification in enhancing synaptic plasticity as well as learning and memory.

Key words: **neurogranin; calmodulin; water maze; learning; LTP; calcium signaling**

Introduction

Neurogranin/RC3 (Ng) is a 78 amino acid neuronal protein that binds calmodulin (CaM) at low level of Ca^{2+} and is implicated in the modulation of Ca^{2+}- and Ca^{2+}–CaM-mediated signaling pathways (Gerendasy and Sutcliffe, 1997; Chakravarthy et al., 1999). This protein is a specific substrate of PKC and is highly concentrated in cytoplasm and dendrites of selective neurons within the forebrain. The phosphorylated Ng binds CaM poorly (Huang et al., 1993, 2000) but can stimulate the G-protein-coupled phosphoinositide second messenger pathways to trigger the mobilization of Ca^{2+} from intracellular stores (ICSs) (Cohen et al., 1993). These combined effects of PKC-mediated phosphorylation of Ng effectively raise the intracellular concentration of Ca^{2+} and Ca^{2+}–CaM to stimulate the Ca^{2+}- and Ca^{2+}–CaM-dependent enzymes. In addition, Ng is susceptible to oxidant-mediated modification, which causes glutathionylation (Li et al., 2001; Huang and Huang, 2002) and/or the formation of intramolecular disulfide bonds (Mahoney et al., 1996; Sheu et al., 1996). Oxidative modification of Ng forming intramolecular disulfide, which functionally resembles the PKC-mediated phosphorylation, also results in a reduction of binding affinity for CaM (Huang et al., 2000). Aside from posttranslational modifications, Ng level in the brain is regulated by thyroid hormone and retinoic acid (Bernal et al., 1992; Iniguez et al., 1992; Etchamendy et al., 2001; Husson et al., 2003) and affected during aging (Iniguez et al., 1992; Enderlin et al., 1997). Both aging and vitamin A deficiency cause a reduction in Ng and are accompanied by selective behavioral impairment (Etchamendy et al., 2001; Mons et al., 2001).

Because Ng has no known enzymatic activity, the mechanism by which this protein modulates the synaptic plasticity and cognitive behavior is not clear. Previously, we demonstrated that $Ng^{-/-}$ mice exhibited severe deficits in performing spatial learning tasks (Pak et al., 2000; Miyakawa et al., 2001). In addition, the agonist-stimulated autophosphorylation of Ca^{2+}/calmodulin-dependent protein kinase II (CaMKII) and activations of PKC and cAMP-dependent protein kinase in hippocampal slices from $Ng^{-/-}$ mice were depressed compared with those of $Ng^{+/+}$ mice (Pak et al., 2000; Wu et al., 2002). However, in our previous studies of high-frequency-induced long-term potentiation (LTP) in the CA1 region of hippocampal slices, using a strong stimulation protocol (3× 100 Hz for 1 sec at 10 min intervals), we did not observe any significant difference between $Ng^{-/-}$ mice and their $Ng^{+/+}$ littermates (Pak et al., 2000). Thus, in this study we pursued the question of whether deletion of Ng affected the induction of LTP and the corresponding increase in intracellular Ca^{2+}

Received June 7, 2004; revised Sept. 9, 2004; accepted Oct. 9, 2004.

*K.-P.H. and F.L.H. contributed equally to this work.

Correspondence should be addressed to Drs. Kuo-Ping Huang or Freesia L. Huang, Building 49, Room 6A36, National Institutes of Health, Bethesda, MD 20892-4510. E-mail: kphuang@helix.nih.gov or fhuang@mail.nih.gov.

DOI:10.1523/JNEUROSCI.2213-04.2004

 0270-6474/04/2410660-10$15.00/0

($[Ca^{2+}]_i$) after applying a mild stimulation protocol (1× 100 Hz for 1 sec). Furthermore, we investigated whether the hippocampal levels of Ng among individual mice exhibited any relationship with their performances in acquiring spatial tasks. Our results support the hypothesis that Ng acts as an enhancer of synaptic plasticity and long-term memory. This is most likely attributable to its high concentration in neurons and its affinity for binding to Ca^{2+}-free CaM, which retards direct interaction of Ca^{2+} with CaM through a "mass action" mechanism and, thus, effectively raises the free $[Ca^{2+}]_i$ to potentiate synaptic responses.

Materials and Methods

Water maze. The use of animals was approved by the National Institute of Child Health and Human Development Animal Care and Use Committee. Wild-type (WT) and Ng mutant mice (3–8 months of age; mixed gender) on a mixed background of 129/Sv × C57BL/6 were housed in groups and maintained on a 12 hr light/dark cycle. To learn the hidden-platform version of the water maze, mice received three blocks (inter-block interval, ~2 hr) of four training trials per day during the light phase for 3 consecutive days. In all trials, mice were allowed to swim until they landed on the platform or 60 sec had elapsed (Pak et al., 2000). At the end of the third day of training, a probe test without the platform was conducted; the time spent in each quadrant and the distances traveled were recorded. The escape latencies attained during each block of learning trial as well as the time spent in the target quadrant of the probe test were plotted for each individual against their hippocampal Ng level and evaluated by linear regression. To determine whether the vision acuity of these animals affects their performances, mice were given four blocks of visible-platform task on 1 d after the probe test. The platform was made visible with a grayish cylinder on top, and its position varied across trials.

Determination of Ng content in the hippocampus. After the behavioral testing, mice were killed under halothane anesthesia, and both hippocampi were quickly removed and stored at –80°C. Each hippocampus was homogenized by sonication in 0.4 ml of buffer (25 mM Tris-Cl, pH 7.5, 1 mM EDTA, 1 mM EGTA, and 1% SDS), and the homogenate was used for protein determination, SDS-PAGE (10–20% gradient gel), and immunoblot analysis. Ng in the blot was quantified by its immunoreactivity using antibody #270 (Huang et al., 1993). A linear relationship between the concentration of purified rat brain Ng (up to 0.2 μg/sample) and immunoreactivity revealed by ECL was established. In each blot, purified Ng at three levels, which had been mixed with the hippocampal extracts (20 μg of protein) from the $Ng^{-/-}$ mice, was used as a standard for quantification of the unknown samples containing the same amount of protein (20 μg). Each sample was analyzed for at least five times, and the intensity of immunoreactive bands was quantified by Fotodyne (Hartland, WI) Gel-Pro analyzer program.

Electrophysiology. Electrophysiological recordings were performed in the CA1 region of the transverse hippocampal slices (400 μm), which were kept in oxygenated artificial CSF (ACSF) (in mM: 124 NaCl, 4.9 KCl, 1.3 $MgSO_4$, 2.5 $CaCl_2$, 1.2 KH_2PO_4, 25.6 $NaHCO_3$, and 10 D-glucose, pH 7.4), at room temperature for 1–2 hr for recovery after slicing. The slices were placed in a submerged-type chamber superfused with oxygenated ACSF at a flow rate of ~2 ml/min. Glass electrodes (1–4 MΩ) filled with ACSF were used for stimulation of Schaffer collateral–commissural fibers as well as for recordings of field EPSPs (fEPSPs) from the stratum radiatum and population spikes from the pyramidal cell layer of the CA1 region, respectively. The slope of the fEPSP and the population spike amplitude (PSA), respectively, were used to measure the potentiation. After establishing a stable baseline, which evoked ~40% of the maximal PSA or fEPSP slope, the slices were subjected to low-frequency stimulation (LFS) of 1 Hz for 15 min, 5 Hz for 3 min, or 10 Hz for 1.5 min (900 pulses each). High-frequency stimulation (HFS; 100 Hz for 1 sec) was delivered with a current that evoked ~30% of the maximal response. The HFS protocol used here consisted of a single train at 100 Hz for 1 sec, which is "milder" than our previous "strong" tetanization protocol (Pak et al., 2000) consisting of three times 100 Hz for 1 sec at 10 min intervals. Potentials were amplified using Axoclamp-2B (Axon Instruments, Union City, CA), digitized by CED Power 1401 (Cambridge Electronic Design, Cambridge, UK), and analyzed using Signal 2 software (Cambridge Electronic Design). Values obtained after LFS and HFS were expressed as percentage of their respective baseline recordings. For comparison of the responses between two groups, the last 10 min blocks of recordings were analyzed by *t* test or Mann–Whitney rank sum test. All values are reported as mean ± SEM.

Confocal calcium imaging. After decapitation and dissection of the brain, ventral transverse hippocampal slices (250-μm-thick) were prepared with a Campden Vibroslice (Campden Instruments, Loughborough, UK) and transferred to oxygenated (95% O_2–5% CO_2) ACSF (in mM: 124 NaCl, 0.75 KCl, 1.3 $MgSO_4$, 2.5 $CaCl_2$, 1.25 KH_2PO_4, 26 $NaHCO_3$, and 10 D-glucose, pH 7.4) kept at 32°C. Pyramidal CA1 neurons and their Ca^{2+} transients were visualized with an Odyssey XL confocal laser-scanning microscope (Noran Instruments, Middleton, WI), mounted on a Zeiss Axioskop-FS upright microscope (Zeiss, Jena, Germany). Image acquisition was done using Intervision software on a Silicon Graphics Indy workstation. All recordings were performed with a 488 nm excitation filter and a 515 nm long-pass emission filter. The slit aperture on the photomultiplier set was adjusted to 100 μm width. A 40× water-immersion objective (numerical aperture, 0.75) was used to visualize neurons. CA1 pyramidal cells were impaled with potassium acetate (2 M)-filled borosilicate glass microelectrodes (Clark, Pangbourne, UK). The tip of this sharp electrode was filled with a 2 mM concentration of the Ca^{2+}-sensitive dye Calcium Green-1 (Molecular Probes, Leiden, The Netherlands). A monopolar stimulating electrode was positioned in CA1 stratum radiatum. Only neurons with a membrane potential more negative than 55 mV [recorded with a SEC 1L-amplifier at bridge-mode (NPI Electronic, Tamm, Germany)] were used. The electrophysiological properties of the neurons were controlled during the entire experiment. The neurons were filled by applying a steady-state hyperpolarizing current of ~100–400 pA for 15–20 min. Only those dendritic regions that were well filled with dye and at a distance of 50–200 μm from soma were chosen for recording the calcium response to different types of stimulation. For recording the calcium response to either a strong HFS (100 Hz, 1 sec, 0.3 msec pulse width) or a weak HFS (100 Hz, 400 msec, 0.3 msec pulse width), the changes in fluorescence intensity were averaged over 66.7 msec (average of eight images). For data analysis, four regions of interests (ROI) were selected on the dendritic tree. The fluorescence intensities of these four ROI were averaged, a background correction was performed, and the results were given as F/F_0, whereby F_0 was the averaged intensity before the tetanization. To pursue changes in $[Ca^{2+}]_i$ during the induction of long-term depression (LTD) by LFS, 900 pulses at 5 Hz were applied, and the corresponding calcium responses were recorded four times (at 0, 1, 2, and 3 min) for 6.67 sec each with a sampling interval of 66.7 msec.

Results

Quantification of hippocampal Ng

To assess the influence of hippocampal Ng content on spatial learning, mice that had been subjected to Morris water maze training were killed, and the individual hippocampal Ng levels were determined by quantitative Western blot. A few representative blots consisting of $Ng^{+/+}$ (W), $Ng^{+/-}$ (H), and $Ng^{-/-}$ (K) along with purified Ng as standard are shown in Figure 1. The Ng content ranged from 1.2 to 2.8 μg/mg in $Ng^{+/+}$ mice and from 0.5 to 1.7 μg/mg protein in $Ng^{+/-}$ mice. On average, the hippocampal Ng in $Ng^{+/+}$ and $Ng^{+/-}$ mice was 1.9 ± 0.39 (SD; n = 46) and 1.1 ± 0.32 (SD; n = 48) μg/mg protein, respectively. $Ng^{-/-}$ mice contained no detectable Ng in Western blot using antibody #270 (against purified rat brain Ng) or three separate peptide antibodies against different regions within the Ng molecule. Based on a molecular weight of 7500, the concentration of Ng in the hippocampus of $Ng^{+/+}$ mice was estimated to be ~260 pmol/mg protein, which is ranked among the highest of all known CaM-binding proteins in the brain. For example, the estimated concentration of neuromodulin/GAP-43 in bovine brain is 0.1–0.5% of the total protein (~40–200 pmol/mg protein)

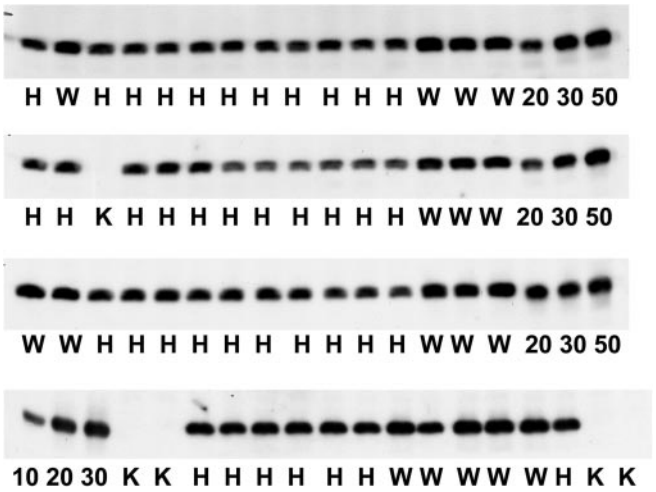

Figure 1. Representative immunoblots of hippocampal Ng of Ng $^{+/+}$, Ng $^{+/-}$, and Ng $^{-/-}$ mice. Hippocampal extracts (20 μg of protein) from Ng $^{+/+}$ (W), Ng $^{+/-}$ (H), and Ng $^{-/-}$ (K) along with purified Ng (10–50 ng) as standard were resolved by 10–20% SDS-PAGE and analyzed by immunoblot with Ng antibody #270. Note that Ng contents among individual Ng $^{+/+}$ and Ng $^{+/-}$ mice are quite variable, and Ng $^{-/-}$ mice contain no Ng.

(Cimler et al., 1985), calcineurin (PP2B) in rat cerebrum is ~140 μg/gm tissue (~10 pmol/mg protein) (Tallant and Cheung, 1983), and CaMKII in rat hippocampus is 2% (~400 pmol/mg) (Erondu and Kennedy, 1985). Considering its localization in the soma and dendrites of selective neurons, the intracellular concentration of Ng in hippocampal neurons of Ng $^{+/+}$ mice is estimated to be, minimally, 65 μM (assuming that the protein content is 0.25 gm/ml cell volume), a concentration that far exceeds that of CaM (20 μM) (Bhalla and Iyengar, 1999).

Relationship between performance in the water maze and hippocampal Ng content

In the hidden-platform version of the Morris water maze, the escape latencies of Ng $^{+/+}$ and Ng $^{+/-}$ mice after training were shorter than those of their Ng $^{-/-}$ littermates across all trials (Fig. 2*A*). The rates of learning of Ng $^{+/+}$ were slightly better than those of Ng $^{+/-}$ mice and significantly greater than those of the Ng $^{-/-}$ mice. Ng $^{+/+}$ mice attained the training criterion (landing at the platform within 20 sec) after the fifth block of training, and Ng $^{+/-}$ mice attained the criterion after the eighth block, whereas Ng $^{-/-}$ mice did not reach this criterion even after the ninth block. It was noted previously that Ng $^{-/-}$ mice displayed anxious behaviors (Miyakawa et al., 2001), which could be the basis of their relatively poor performances in various spatial tasks. These behavioral traits, however, were not evident among Ng $^{+/+}$ and Ng $^{+/-}$ mice. Because the hippocampal Ng contents among individual Ng $^{+/+}$ and Ng $^{+/-}$ mice varied widely, we attempted to determine whether there was any correlation between the level of Ng and the performance of each individual across different blocks of trial. For Ng $^{+/+}$ mice ($n = 46$), the linear regression of the escape latency versus hippocampal Ng content was nearly horizontal for all the training blocks ($r < 0.3$), although there was trend for those individuals having higher Ng levels to perform the task better (data not shown). Likewise, learning performance of Ng $^{+/-}$ mice ($n = 48$) also showed a nearly horizontal slope of the regression line for the first block of trial (Fig. 2*B*), suggesting the absence of any influence of Ng level on performance when mice were first subjected to the task. In the subsequent trials, however, negative slopes could be observed, being most prominent at the

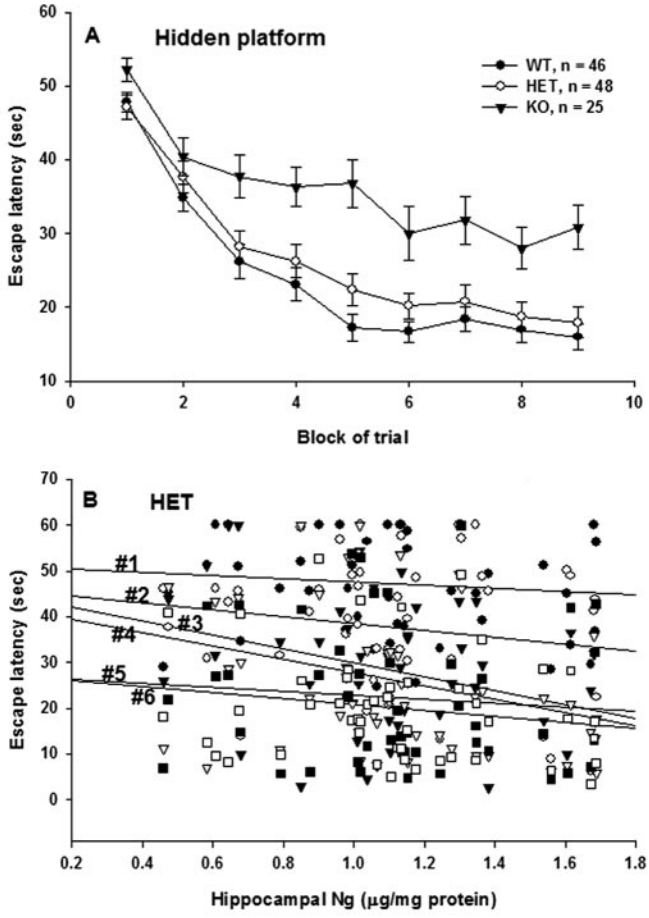

Figure 2. Performance of Ng $^{+/+}$, Ng $^{+/-}$, and Ng $^{-/-}$ mice in the hidden-platform task of the Morris water maze and their hippocampal Ng levels. *A*, Escape latency of Ng $^{+/+}$ (WT; $n = 46$), Ng $^{+/-}$ [heterozygotes (HET); $n = 48$], and Ng $^{-/-}$ [knock-out (KO); $n = 25$] in the hidden-platform trial of the Morris water maze. Ng $^{+/+}$ and Ng $^{+/-}$ mice attain the training criterion of reaching the platform in 20 sec after the fifth and eighth block, respectively, whereas Ng $^{-/-}$ mice fail to reach this criterion even after the ninth block. *B*, Linear regression of the escape latency versus hippocampal Ng level was compiled for the first six blocks of learning sessions for Ng $^{+/-}$ mice ($n = 48$). Relationship between hippocampal Ng level and performance of mice in the hidden-platform task was evaluated from the slope of the regression curves. For Ng $^{+/-}$ mice, linear regression lines for blocks 1, 2, 5, and 6 were near horizontal ($r < 0.3$), and negative slopes were more prominent at the third ($r = 0.33$) and fourth ($r = 0.3$) block. *B*, Symbols: ●, block 1; ○, block 2; ▼, block 3; ▽, block 4; ■, block 5; □, block 6.

third ($r = 0.33$) and fourth ($r = 0.3$) block (Fig. 2*B*). From the fifth to the ninth block, linear regression curves again became nearly horizontal and exhibited only small improvement in performance (data not shown for the seventh to the ninth block). Comparing learning of the hidden-platform tasks (escape latency vs block of trial) of Ng $^{+/+}$ and Ng $^{+/-}$ mice at two chosen levels, high Ng (>75th percentile among test subjects) and low Ng (<25th percentile among test subjects), we determined that there was a significant relationship between hippocampal Ng levels and learning performances of the heterozygotes (Fig. 3). It seems that the two learning curves of Ng $^{+/+}$ mice (Fig. 3*A*) reflect a "ceiling" effect of Ng on learning performance (i.e., their hippocampi contain Ng levels near or over a critical threshold that is required for normal spatial learning). This might explain the lack of statistical differences between the "low-Ng" and "high-Ng" groups. For Ng $^{+/-}$ mice, a significantly improved rate of learning was seen in the "high-Ng" compared with the "low- Ng" group; training criterion were obtained at the fourth and eighth block, respectively

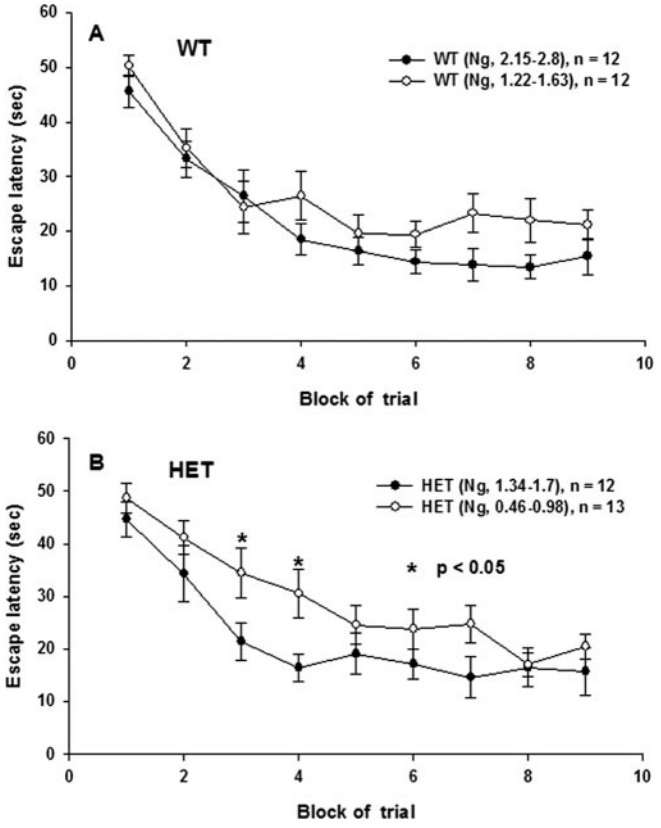

Figure 3. Comparison of the performances of high and low hippocampal Ng groups among Ng $^{+/+}$ and Ng $^{+/-}$ mice in hidden-platform trial. *A*, Rates of learning (acquisition) among Ng $^{+/+}$ mice having high and low Ng levels. Although the Ng $^{+/+}$ (WT) mice having high Ng levels (75th percentile; 2.15–2.8 μg/mg; $n = 12$; -●-) displayed a tendency of having shorter escape latencies than those having low Ng (25th percentile; 1.22–1.63 μg/mg; $n = 12$; -○-), the differences between these two groups were not statistically significant. *B*, Rates of learning (acquisition) among Ng $^{+/-}$ mice having high and low Ng levels. In blocks 3 and 4, Ng $^{+/-}$ [heterozygotes (HET)] mice having high Ng levels (75th percentile; 1.34–1.7 μg/mg; $n = 12$; -●-) performed significantly better than those having low Ng levels (25th percentile; 0.46–0.98 μg/mg; $n = 13$; -○-). Thus, after having adapted to the training protocol, the high-Ng group of Ng $^{+/-}$ mice displayed a faster learning than the low-Ng group.

(Fig. 3*B*). These findings indicate that increasing hippocampal Ng levels exert a beneficial effect on the spatial learning among Ng $^{+/-}$ mice.

After the ninth block of trial, mice were subjected to the probe test, during which the platform is removed and the animal is scored for its preference to the quadrant of the former platform location. On average, Ng $^{+/+}$ mice spent more time in the target quadrant (42.3 ± 2.36%; $n = 44$) than Ng $^{+/-}$ (34.91 ± 2.46%; $n = 37$) and Ng $^{-/-}$ (30 ± 2.79%; $n = 25$) mice (Fig. 4*A*). The genotype differences were significant for Ng $^{+/+}$ versus Ng $^{-/-}$ (*t* test; $t = 3.25$; $p < 0.05$) and Ng $^{+/+}$ versus Ng $^{+/-}$ (*t* test; $t = 2.17$; $p < 0.05$), but not significant for Ng $^{+/-}$ versus Ng $^{-/-}$ (*t* test; $t = 1.28$; $p = 0.206$). The linear regression curve of the time spent in the target quadrant versus the hippocampal Ng content of individual mice showed a steeper positive slope for Ng $^{+/-}$ ($r = 0.41$; ANOVA; $F = 6.96$) than that of Ng $^{+/+}$ ($r = 0.27$; ANOVA; $F = 2.27$) mice (Fig. 4*B*). These findings indicate that there is a positive correlation between the performances of the mice in the probe test and their hippocampal Ng contents, especially for Ng $^{+/-}$ mice. Again, by segregating the mice into high-Ng (>75th percentile) and low-Ng (<25th percentile) groups among Ng $^{+/+}$ (2.15–2.8 and 1.22–1.63 μg/mg) and Ng $^{+/-}$ (1.34–1.7 and 0.46–0.98 μg/mg) animals, it was evident that the high-Ng groups

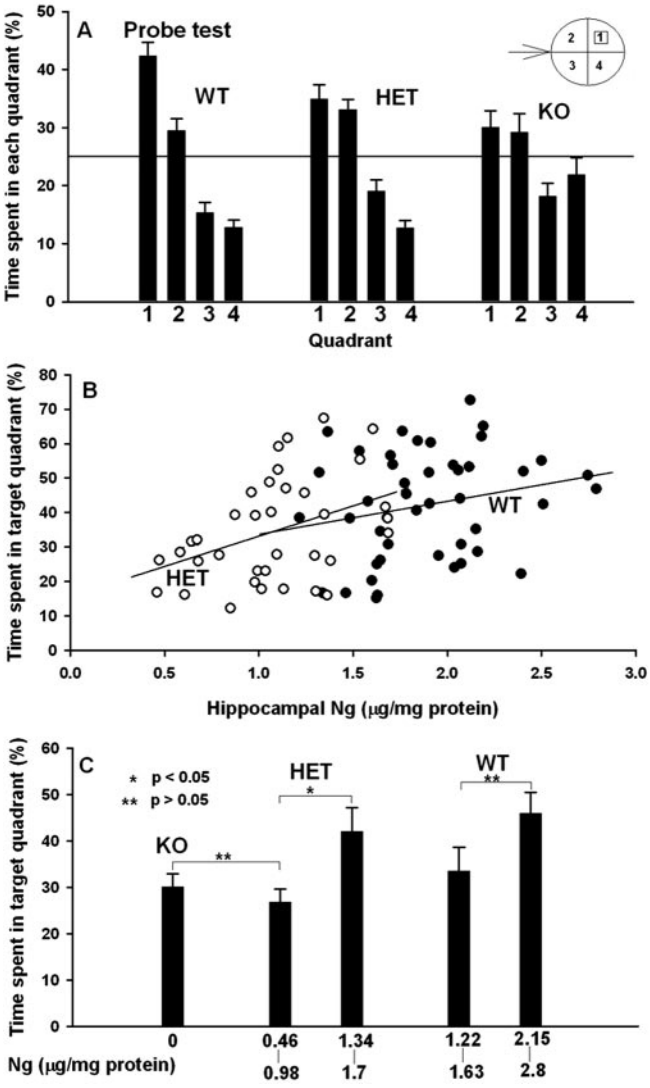

Figure 4. Correlation between the hippocampal Ng level and performance of the probe test. *A*, Time spent in each quadrant during the probe test. Percentage of time each group of mice spent in the target quadrant (#1) was as follows: Ng $^{+/+}$ (WT), 42.3 ± 2.36%, $n = 44$; Ng $^{+/-}$ [heterozygote (HET)], 34.91 ± 2.46%, $n = 37$; and Ng $^{-/-}$ [knock-out (KO)], 30 ± 2.79%, $n = 25$. The genotype differences were significant for Ng $^{+/+}$ versus Ng $^{-/-}$ (*t* test; $t = 3.25$; $p < 0.05$) and Ng $^{+/+}$ versus Ng $^{+/-}$ (*t* test; $t = 2.17$; $p < 0.05$) but not significant for Ng $^{+/-}$ versus Ng $^{-/-}$ (*t* test; $t = 1.28$; $p = 0.206$). *B*, Linear regression of the time spent in the target quadrant versus the hippocampal Ng level of individual mice. The slope for Ng $^{+/-}$ ($r = 0.41$; ANOVA; $F = 6.96$) was greater than that of Ng $^{+/+}$ ($r = 0.27$; ANOVA; $F = 2.27$) mice. *C*, Performances of Ng $^{+/+}$ and Ng $^{+/-}$ mice having different hippocampal Ng levels in the probe test. Those Ng $^{+/+}$ and Ng $^{+/-}$ mice having high Ng (Ng $^{+/+}$, 2.15–2.80 μg/mg; Ng $^{+/-}$, 1.34–1.70 μg/mg) performed better than their respective low Ng groups (Ng $^{+/+}$, 1.22–1.63 μg/mg; Ng $^{+/-}$, 0.46–0.98 μg/mg). The differences among these high-Ng and low-Ng groups were as follows: Ng $^{+/+}$, high, 46 ± 4.4% ($n = 10$) versus low, 33.6 ± 5.1% ($n = 12$), *t* test, $t = 1.8$, $p = 0.086$; and Ng $^{+/-}$, high, 42.1 ± 5.1% ($n = 10$) versus low, 26.9 ± 2.8% ($n = 12$), *t* test, $t = 2.7$, $p < 0.05$. The low-Ng group of Ng $^{+/-}$ mice performed as poorly as Ng $^{-/-}$ mice.

performed better than those of the low-Ng groups (Ng $^{+/+}$, 46 ± 4.4%, $n = 10$ vs 33.6 ± 5.1%, $n = 12$; Ng $^{+/-}$, 42.1 ± 5.1%, $n = 10$ vs 26.9 ± 2.8%, $n = 12$) (Fig. 4*C*). The differences between high- and low-Ng groups were greater in Ng $^{+/-}$ mice (*t* test; $t = 2.7$; $p < 0.05$) compared with Ng $^{+/+}$ mice (*t* test; $t = 1.8$; $p = 0.086$). The low-Ng group of Ng $^{+/-}$ performed as poorly as Ng $^{-/-}$; this is in contrast to the learning during hidden-platform trial, in which the Ng $^{+/-}$ low-Ng group performed better than

$Ng^{-/-}$ (Fig. 3*B*, compare low-Ng group with $Ng^{-/-}$ in Fig. 2*A*). These observations suggest that the normal learning during the hidden-platform trial and the probe test differ in their critical Ng threshold. The probe test, compared with the hidden-platform trial, apparently is more demanding and has a higher hippocampal Ng threshold level for achieving better performance. The differences in performance among the high-Ng and low-Ng groups within $Ng^{+/+}$ and $Ng^{+/-}$, as well as those of $Ng^{-/-}$ mice, were not attributable to differences in their swimming speeds, ranging from 18 to 21 cm/sec for the three genotypes. The escape latencies of these mice in the visible-platform task after the probe test were also comparable ($Ng^{+/+}$, 5.4 ± 0.54 sec, $n = 21$; $Ng^{+/-}$, 7.7 ± 1.8 sec, $n = 11$; and $Ng^{-/-}$, 5.1 ± 0.34 sec, $n = 14$), suggesting that the differences in performing learning and memory tasks among them are not caused by altered vision.

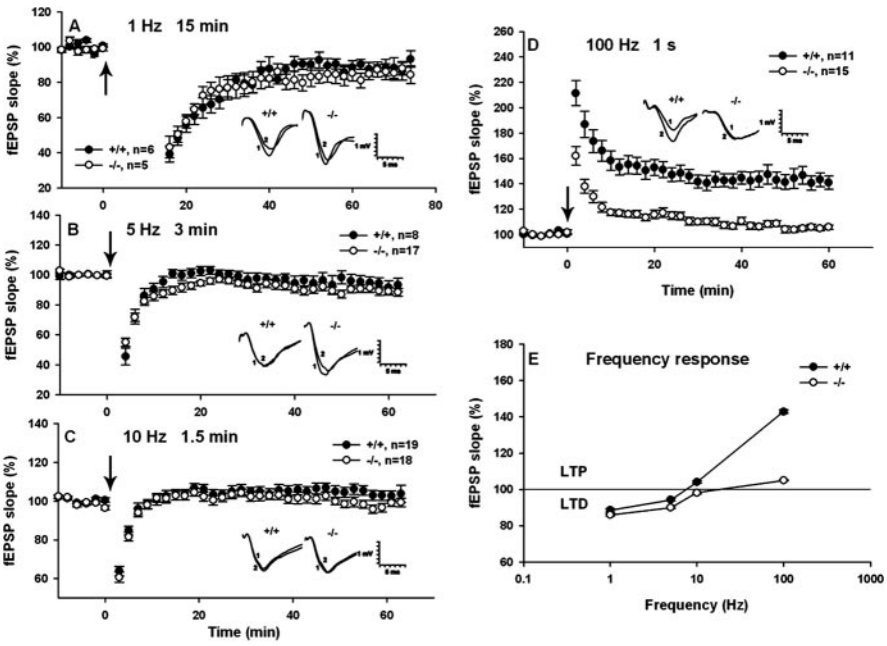

Figure 5. Frequency–responses of the fEPSP slope of adult $Ng^{+/+}$ and $Ng^{-/-}$ mice obtained by stimulation at 1, 5, 10, and 100 Hz. Hippocampal slices from $Ng^{+/+}$ and $Ng^{-/-}$ mice were stimulated with 900 pulses at time 0 (indicated by the arrow) with 1 Hz (*A*), 5 Hz (*B*), and 10 Hz (*C*) or 100 pulses at 100 Hz (*D*) after establishing a stable baseline. The slope of fEPSP was determined. The steady-state levels of responses between $Ng^{+/+}$ and $Ng^{-/-}$ mice during the last 10 min blocks were as follows (percentage of mean ± SEM of baseline): 1 Hz, $Ng^{+/+}$, 89.7 ± 0.9% ($n = 6$) versus $Ng^{-/-}$, 84.9 ± 0.6% ($n = 5$); 5 Hz, $Ng^{+/+}$, 94.8 ± 0.9% ($n = 8$) versus $Ng^{-/-}$, 89.8 ± 0.5% ($n = 17$); 10 Hz, $Ng^{+/+}$, 104.6 ± 0.5% ($n = 19$) versus $Ng^{-/-}$, 99.1 ± 0.6% ($n = 18$); and 100 Hz, $Ng^{+/+}$, 143.4 ± 0.7% ($n = 11$) versus $Ng^{-/-}$, 106 ± 0.5% ($n = 15$). The frequency–response curve of $Ng^{-/-}$ mice exhibited a decrease in LTP induction with minimal effect on LTD compared with those of the $Ng^{+/+}$ (*E*). Representative traces of fEPSP before (trace 1) and 60 min after (trace 2) of recording are shown. Calibration: 1 mV, 5 msec.

Differences in electrophysiological responses between $Ng^{+/+}$ and $Ng^{-/-}$ mice

Autophosphorylation of CaMKII has been implicated in the potentiation of synaptic response by organizing neurotransmitter receptor assembly (Lisman and Zhabotinsky, 2001; Lisman et al., 2002) and contributes to learning and memory of spatial tasks (Silva et al., 1992; Giese et al., 1998). We have shown previously that $Ng^{-/-}$ mice contained a lower level of the autophosphorylated CaMKII in the hippocampus and exhibited deficits in the autophosphorylation of this kinase when treated with the protein phosphatase (PP) inhibitor okadaic acid or the NO donor sodium nitroprusside (Pak et al., 2000). However, with the "strong" induction protocol for LTP used in the previous study (3× 100 Hz for 1 sec at 10 min intervals), $Ng^{+/+}$ and $Ng^{-/-}$ mice exhibited only minor differences in the EPSP component of LTP (Pak et al., 2000). Here, we tested the expression of LTP in hippocampal slices from $Ng^{+/+}$ and $Ng^{-/-}$ mice by HFS under a "milder" condition (only 1× 100 Hz for 1 sec) and also determined their synaptic responses to LFS (Fig. 5). Under such condition, the expression of LTP measured by the fEPSP slope differed significantly between the $Ng^{+/+}$ (143.4 ± 0.7%; $n = 11$) and $Ng^{-/-}$ (106 ± 0.5%; $n = 15$) mice (*t* test; $t = 41.95$; $p \leq 0.001$) (Fig. 5*D*), indicating a severe deficit in the ability of $Ng^{-/-}$ mice to express this type of HFS-induced LTP. When stimulated for 900 pulses at 1, 5, and 10 Hz, slices from $Ng^{+/+}$ mice exhibited slightly greater responses than those from $Ng^{-/-}$ mice (1 Hz: $Ng^{+/+}$, 89.7 ± 0.9%, $n = 6$ vs $Ng^{-/-}$, 84.9 ± 0.6%, $n = 5$; 5 Hz: $Ng^{+/+}$, 94.8 ± 0.9%, $n = 8$ vs $Ng^{-/-}$, 89.8 ± 0.5%, $n = 17$; and 10 Hz: $Ng^{+/+}$, 104.6 ± 0.5%, $n = 19$ vs $Ng^{-/-}$, 99.1 ± 0.6%; $n = 18$) (Fig. 5*A–C*). When the data are compiled as a frequency–response, it is evident that $Ng^{-/-}$ mice displays a decrease in LTP induction with a minor effect on LTD.

Induction of LTP by HFS of CA1 apical dendrites results in a potentiation not only of the fEPSP slope but also of the PSA, which is usually larger in terms of percentage than the increase in the fEPSP slope. To confirm the results seen in the EPSP component of LTP, we also investigated the tetanus-induced changes in the PSA of CA1 neurons in $Ng^{+/+}$ and $Ng^{-/-}$ mice (Fig. 6). Despite the meager LTP of the fEPSP in $Ng^{-/-}$ slices (Fig. 5), the same tetanus (1× 100 Hz for 1 sec) induced sizable LTP of PSA with an initial magnitude of 223 ± 6.8% and a remaining potentiation of 137 ± 3.2% ($n = 7$) 60 min after tetanization. However, this potentiation was again significantly lower than that of $Ng^{+/+}$ mice (181 ± 3.9%; 60 min after tetanus; $n = 9$) (*t* test; $t = 8.41$; $p < 0.001$) (Fig. 6*D*). Interestingly, the initial magnitude of LTP of $Ng^{+/+}$ was only slightly higher (244 ± 7.4%) than that of mutant mice. After the establishment of LTP (60 min after 100 Hz for 1 sec), application of LFS at 1 Hz for 15 min caused depotentiation in slices from both $Ng^{+/+}$ and $Ng^{-/-}$ mice (at 75 min: $Ng^{+/+}$, 60.5 ± 8.5% of pre-100 Hz baseline, $n = 6$ vs $Ng^{-/-}$, 45.2 ± 9.3%, $n = 4$) followed by a gradual recovery during the subsequent 60 min to a steady-state level below their respective LTP response ($Ng^{+/+}$, 142.8 ± 0.71, $n = 6$ vs $Ng^{-/-}$, 128.9 ± 1.57, $n = 4$; $t = 8.12$; $p < 0.001$, for the last 10 min response) (data not shown). These results indicate that the PSA LTP of $Ng^{-/-}$ can also be depotentiated like that of $Ng^{+/+}$ mice. Application of the same LFS (900 pulses at 1 Hz for 15 min) to naive $Ng^{+/+}$ and $Ng^{-/-}$ hippocampal slices resulted in a greater depression of $Ng^{-/-}$ than that of $Ng^{+/+}$ slices (Fig. 6*A*) (79 ± 1.8 vs 87 ± 0.8% of baseline response; $t = -4.26$; $p < 0.001$). The steady-state level of responses after stimulation of the $Ng^{+/+}$ and $Ng^{-/-}$ slices with 5 Hz for 3 min (Fig. 6*B*) (103 ± 1.7 vs 87 ± 1.2%; $t = 6.37$; $p < 0.001$) and 10 Hz for 1.5 min (Fig. 6*C*) (113 ± 2.2 vs 94 ± 1.6%; $t = 6.71$; $p < 0.001$) generated modest levels of LTP in the

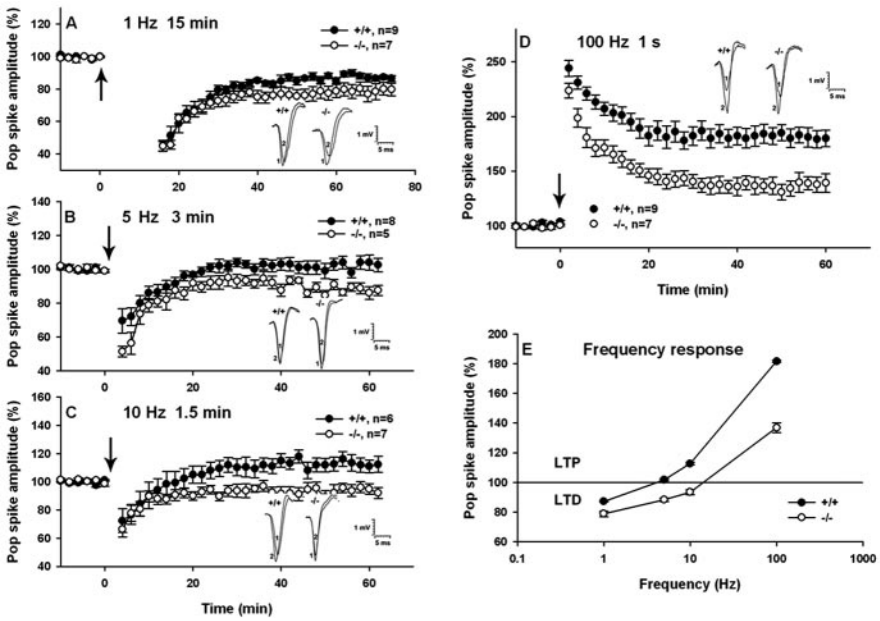

Figure 6. Frequency–responses of the population spike amplitude of adult $Ng^{+/+}$ and $Ng^{-/-}$ mice by stimulation at 1, 5, 10, and 100 Hz. After establishing a stable baseline, hippocampal slices were stimulated with 900 pulses each at time 0 (indicated by the arrow) with 1 Hz (*A*), 5 Hz (*B*), and 10 Hz (*C*) or with 100 pulses at 100 Hz (*D*). The steady-state level of responses during the last 10 min of recording between $Ng^{+/+}$ and $Ng^{-/-}$ mice was compared, and the magnitude of population spike was as follows (% mean ± SEM of baseline): 1 Hz, $Ng^{+/+}$, 87 ± 0.8% ($n = 9$) versus $Ng^{-/-}$, 79 ± 1.9% ($n = 7$); 5 Hz, $Ng^{+/+}$, 103 ± 1.7% ($n = 8$) versus $Ng^{-/-}$, 87 ± 1.3% ($n = 5$); 10 Hz, $Ng^{+/+}$, 113 ± 2.3% ($n = 6$) versus $Ng^{-/-}$, 94 ± 1.6% ($n = 7$); and 100 Hz, $Ng^{+/+}$, 181 ± 3.9% ($n = 9$) versus $Ng^{-/-}$, 137 ± 3.2% ($n = 7$). Stimulation with 1 Hz induced LTD in both the $Ng^{+/+}$ and $Ng^{-/-}$, whereas 5 and 10 Hz stimulations induced modest LTP in $Ng^{+/+}$ mice but LTD in $Ng^{-/-}$ mice, and 100 Hz induced LTP in both $Ng^{+/+}$ and $Ng^{-/-}$ mice. The frequency–response curve of $Ng^{-/-}$ shifts to the right compared with $Ng^{+/+}$ (*E*). Insets show population spikes recorded before (1) and 60 min after (2) stimulation, respectively.

$Ng^{+/+}$ but caused LTD for the $Ng^{-/-}$. The PSA frequency–response curve of the $Ng^{-/-}$ displayed a shift to the right (Fig. 6*E*) that is more pronounced over the entire range of frequencies compared with that of the EPSP responses. It seems that the Ng-mediated signal transduction mechanisms of activity-dependent increases in synaptic efficacy and excitability are different (i.e., the effects on excitability at the soma appear to be amplified to a greater extent).

The frequency between 5 and 12 Hz is of particular physiological relevance, because it is known that hippocampal neurons of adult rodents fire at this frequency range during active exploration of a novel environment (Paulsen and Sejnowski, 2000). Therefore, we studied the synaptic responses of $Ng^{+/+}$ and $Ng^{-/-}$ mice during and immediately after 10 Hz stimulation in more detail (Fig. 7). During the course of 10 Hz stimulation (sampling at 20 sec intervals), both $Ng^{+/+}$ and $Ng^{-/-}$ slices exhibited the same kinetics of synaptic fatigue (depression at 80 sec after stimulation: $Ng^{+/+}$, 17.8 ± 1.7%, $n = 9$ vs $Ng^{-/-}$, 14.2 ± 2.2%, $n = 13$; *t* test; $t = 1.18$; $p = 0.25$) (Fig. 7*A*). Interestingly, at 90 sec after onset of 10 Hz stimulation, the potentials of both $Ng^{+/+}$ and $Ng^{-/-}$ mice were recovered transiently to ~80–90% of baseline responses before undergoing another larger depression (e.g., at 140 sec: $Ng^{+/+}$, 66.3 ± 5.6% vs $Ng^{-/-}$, 44.5 ± 3.6% of baseline response), followed by a gradual recovery to near baseline level. The extent of depression in the $Ng^{-/-}$ slices was significantly greater than that of the $Ng^{+/+}$ slices. Sampling of the responses at 10 Hz for 1 sec (100 msec interpulse intervals) did not reveal any significant difference between the two genotypes (i.e., both exhibited a similar degree of potentiation at the second pulse [paired-pulse facilitation (PPF), $Ng^{+/+}$, 128.7 ± 2.8%, $n = 7$ vs $Ng^{-/-}$, 132 ± 2.4%, $n = 7$] followed by a gradual decline) (Fig. 7*B*). These results indicate that during 10 Hz stimulation, presynaptic mechanisms, as reflected by the paired-pulse facilitation and synaptic fatigue, are indistinguishable between $Ng^{+/+}$ and $Ng^{-/-}$. However, the greater post-tetanic depression seen in the $Ng^{-/-}$ slices is likely caused by an attenuated postsynaptic response in the absence of Ng.

Confocal calcium imaging

The attenuated responses of $Ng^{-/-}$ mice to tetanic stimulation could result from a functional deficit of any signaling pathway involved in the induction and maintenance of LTP. However, many of these pathways share the property of being triggered by an initial increase in free $[Ca^{2+}]_i$ which is accomplished either by Ca^{2+} influx through NMDA receptors (NMDARs) and voltage-gated Ca^{2+} channels or by Ca^{2+} release from ICSs. Therefore, it was tempting to determine whether the impaired LTP in $Ng^{-/-}$ is caused by altered $[Ca^{2+}]_i$ kinetics during tetanic stimulation. CA1 pyramidal neurons were loaded with the fluorescence Ca^{2+} indicator Calcium Green-1 and stimulated by a monopolar stimulating electrode positioned ~50–200 μm apart from the soma in CA1 stratum radiatum. As depicted in Figure 8, tetanizations with a single train at 100 Hz for either 400 or 1000 msec evoked Ca^{2+} transients in proximal dendrites that lasted longer than the duration of HFS. Increasing the duration of tetanization from 400 to 1000 msec resulted in a broadening of the maximum but did not increase the amplitude. However, with both types of tetanization, the increase in the amplitudes of the fluorescence intensity of wild types was approximately twice as high as those of the mutants (400 msec: $Ng^{-/-}$, 1.44 ± 0.09, $n = 7$; $Ng^{+/+}$, 1.69 ± 0.17, $n = 5$; 1000 msec: $Ng^{-/-}$, 1.50 ± 0.1, $n = 7$; $Ng^{+/+}$, 1.95 ± 0.13, $n = 5$; $p < 0.05$; Mann–Whitney *U* test). Although the transients evoked by the 400 msec tetanus decayed earlier, their decay time constant tau, determined by a nonlinear fit of a one-phase exponential equation ($y = a * e^{-t/\mathrm{tau}} + b$), did not differ from the 1000 msec tetanus (Fig. 8*B*). Furthermore, tau values were the same for $Ng^{-/-}$ under both stimulation conditions. Because the Ca^{2+} transients are more accurately represented by their integrated area than by their amplitudes (Wilsch et al., 1998), we compared the area F/F_0 of $Ng^{-/-}$ and $Ng^{+/+}$ in response to both types of tetani. As shown in Figure 8*C*, the areas of wild types clearly exceeded those of the mutants (400 msec: $Ng^{-/-}$, 6.78 ± 1.40, $n = 7$; $Ng^{+/+}$, 16.80 ± 4.67, $n = 4$; 1000 msec: $Ng^{-/-}$, 11.50 ± 3.65, $n = 7$; $Ng^{+/+}$, 28.4 ± 6.50, $n = 4$; $p < 0.05$; Mann–Whitney *U* test). During LFS of 5 Hz for 3 min, wild types displayed a trend toward a larger rise-time constant [nonlinear fit of a one-phase exponential equation: $y = a * (1 - e^{-t/\mathrm{tau}}) + b$; $Ng^{+/+}$, 1.56 ± 0.54 sec, $n = 3$; $Ng^{-/-}$, 0.41 ± 0.108 sec, $n = 5$] and a higher initial $[Ca^{2+}]_i$ amplitude than the mutant (Fig. 9*A*,*B*). One minute after the onset of LFS, $[Ca^{2+}]_i$ of both $Ng^{+/+}$ and $Ng^{-/-}$ returned to their respective baseline levels and remained constant thereafter up to 3 min. These findings suggest that binding of Ng to CaM in $Ng^{+/+}$ mice produces a greater increase in the free Ca^{2+} level after HFS compared with that of the $Ng^{-/-}$ without Ng to buffer CaM,

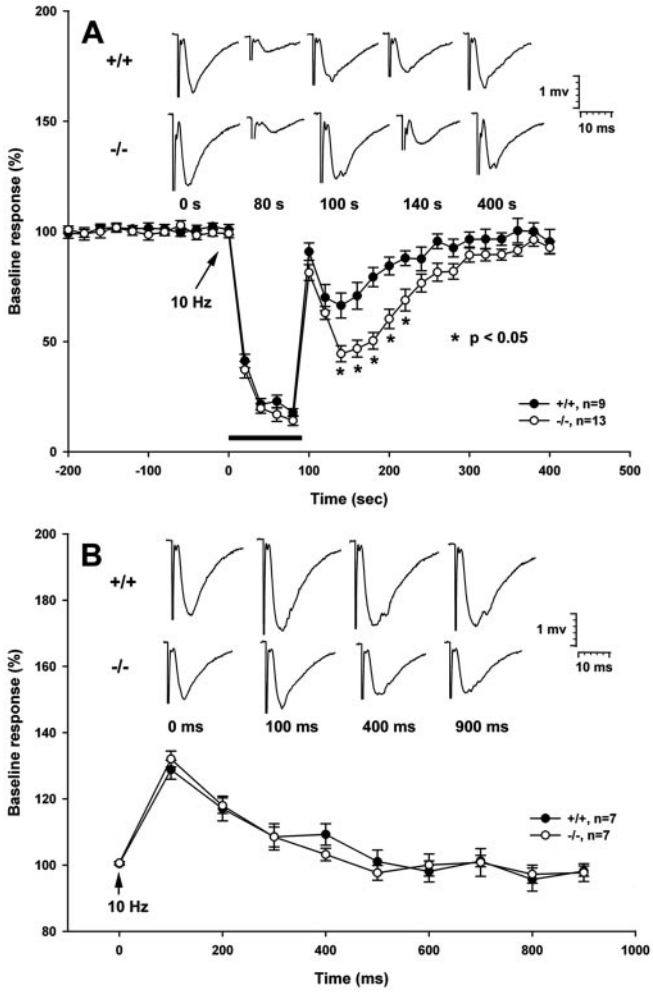

Figure 7. Synaptic responses during and after 10 Hz stimulation. *A*, $Ng^{+/+}$ ($n = 9$) and $Ng^{-/-}$ ($n = 13$) hippocampal slices were stimulated at 10 Hz for 90 sec (underline), and the fEPSP slopes were measured at 20 sec intervals. $Ng^{-/-}$ and $Ng^{+/+}$ exhibited the same decay kinetics (synaptic fatigue) during 10 Hz stimulation and similar levels of transient rebounce after completion of stimulation (~80–90% of baseline at 100 sec). Afterward, $Ng^{-/-}$ underwent a greater depression than $Ng^{+/+}$ [e.g., at 140 sec, WT, 66.3 ± 5.6% vs knock-out (KO), 44.5 ± 3.6%], followed by a gradual recovery to near baseline level. Representative traces of fEPSPs before (0 sec) and after (80, 100, 140, and 400 sec) 10 Hz stimulations are shown. *B*, Recordings during the first second of 10 Hz stimulation. Both genotypes exhibited the same level of PPF and synaptic fatigue. Insets show analog potential traces before (0 msec) and after (100, 400, and 900 msec) application of 10 Hz.

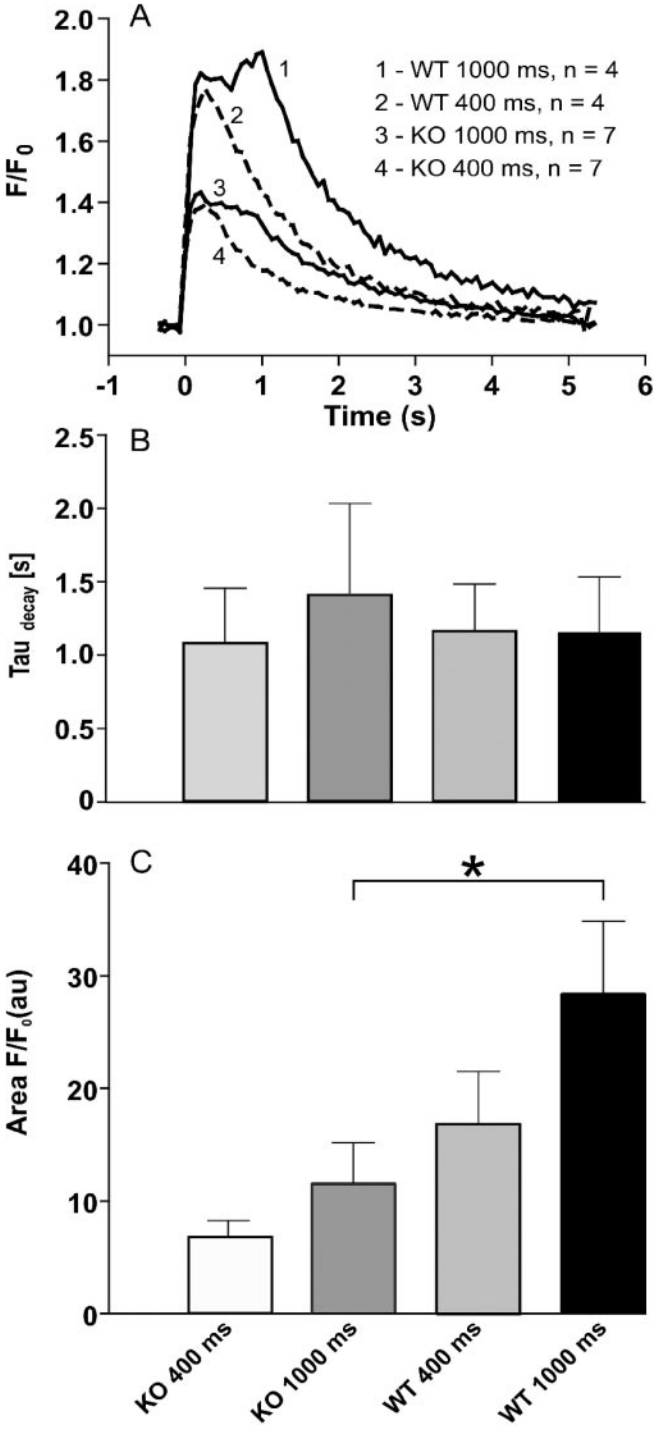

Figure 8. Tetanic stimulation-induced Ca^{2+} responses in hippocampal CA1 neurons from $Ng^{+/+}$ and $Ng^{-/-}$ mice. *A*, Normalized Ca^{2+} transients for $Ng^{+/+}$ (WT, traces 1 and 2) and $Ng^{-/-}$ [knock-out (KO), traces 3 and 4] hippocampal slices evoked by HFS at 100 Hz for 400 msec (traces 2 and 4) and 1000 msec (traces 1 and 3). Note the clear-cut reduction in the amplitude of Ca^{2+} responses in $Ng^{-/-}$ mice. *B*, The decay time constant, tau, of the Ca^{2+} transients of $Ng^{+/+}$ and $Ng^{-/-}$ slices after stimulations for 400 or 1000 msec. Designation of the columns are the same as in *C*. *C*, Ca^{2+} responses expressed as averaged total areas of individual Ca^{2+} transients [given as arbitrary units (au)]. The areas of $Ng^{+/+}$ mice were nearly twice as much as those of $Ng^{-/-}$ under both conditions.

and consequently results in a higher degree of potentiation for $Ng^{+/+}$ mice. The data obtained during LFS stimulation indicate differences in the $[Ca^{2+}]_i$ kinetics during the onset of stimulation, which might be the reason for the increasing propensity of $Ng^{-/-}$ to undergo LTD.

Discussion

How can Ng modulate neuronal Ca^{2+} transients, alter the stimulation threshold to induce LTP and LTD, and, in turn, affect cognitive function? We rationalize that a high intracellular concentration of Ng (>60 μM), as in $Ng^{+/+}$ mice, favors the formation of an Ng–CaM complex at a basal level of $[Ca^{2+}]_i$. After synaptic stimulation, the influxed Ca^{2+} will replace Ng from the complex to form Ca^{2+}–CaM. For this equilibrium, at any given Ca^{2+} influx, a higher Ng concentration will result in higher free $[Ca^{2+}]_i$ through a "mass action" mechanism (supplemental material, available at www.jneurosci.org). An increase in $[Ca^{2+}]_i$ over a certain threshold level is required for the activation of Ca^{2+}- and Ca^{2+}–CaM-dependent signaling cascades, including PKC, CaMKII, adenylyl cyclases 1 and 8, and their downstream targets, such as extracellular signal-regulated kinase (ERK) and

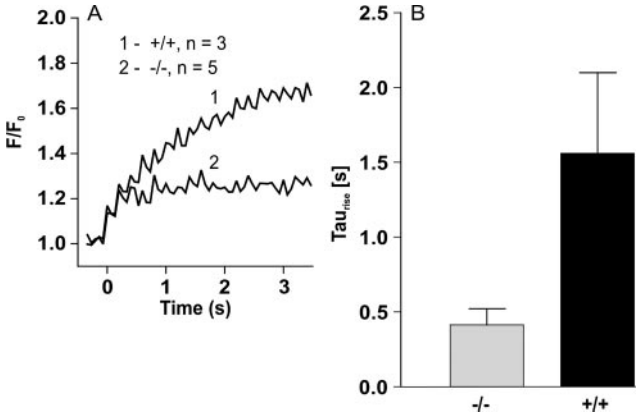

Figure 9. Ca^{2+} responses in hippocampal CA1 neurons from $Ng^{+/+}$ and $Ng^{-/-}$ mice after low-frequency stimulation. During LFS of 5 Hz for 3 min, wild types displayed a trend toward a higher initial $[Ca^{2+}]_i$ amplitude and a larger rise-time constant than the mutant. *A*, Normalized Ca^{2+} transients for $Ng^{+/+}$ ($n = 3$) and $Ng^{-/-}$ ($n = 5$). *B*, Rise-time constant tau obtained by a nonlinear fit of a one-phase exponential equation: $y = a * (1 - e^{-t/tau}) + b$; $Ng^{+/+}$, 1.56 ± 0.54 sec, $n = 3$; $Ng^{-/-}$, 0.41 ± 0.108 sec, $n = 5$.

cAMP response element-binding protein (CREB). Phosphorylation of these signaling components is required for the acquisition and storage of memory (Impey et al., 1999; Wong et al., 1999; Winder and Sweatt, 2001). In addition, stimulated PKC will also activate type 2 and 7 adenylyl cyclases, leading to a greater increase in cAMP level (Tang and Hurley, 1998), and upregulate NMDARs to promote additional Ca^{2+} influx (Zheng et al., 1999). PKC-phosphorylated Ng, which stimulates the G-protein-coupled phosphoinositide pathways, also triggers Ca^{2+} release from the internal stores to increase $[Ca^{2+}]_i$ (Cohen et al., 1993). In the absence of Ng, as in our $Ng^{-/-}$ mice, the influxed Ca^{2+} in the postsynaptic sites is predominantly sequestered by CaM (~20 μM) to form Ca^{2+}–CaM, which results in low free $[Ca^{2+}]_i$ and an attenuated synaptic response. The decreasing propensity in LTP induction (Fig. 5) and the right shift in the frequency–response curve (Fig. 6) of $Ng^{-/-}$ mice compared with those of the $Ng^{+/+}$ mice is consistent with the observed role of Ng in increasing Ca^{2+} transients (Fig. 8) and promoting Ca^{2+}-mediated signaling. The experimental results presented here provide the first demonstration that tetanic stimulation to hippocampal slices induces a more robust neuronal Ca^{2+} transient in the presence of Ng than without this protein. Because the levels and kinetics of $[Ca^{2+}]_i$ after synaptic stimulation dictate the type of plasticity (LTP or LTD) that is induced (Lisman, 2001), it is reasonable to assume that the higher the level of Ng, the greater the increase in $[Ca^{2+}]_i$, which will enhance the propensity to express LTP.

Ng has been shown to be rapidly phosphorylated by PKC and oxidized to form intramolecular disulfides after activation of NMDA receptor (Li et al., 1999; Wu et al., 2003). Both phosphorylation and oxidation of Ng reduce its binding affinity for CaM and thus promote a prolonged increase in Ca^{2+}–CaM even after reduction of $[Ca^{2+}]_i$ to the basal level. Thus termination of the increase in Ca^{2+}–CaM will also be regulated by dephosphorylation of PO_4-Ng by PP1, PP2A, and PP2B (Seki et al., 1995) and by reduction of oxidized Ng by an enzyme system using NADPH (Li et al., 1999). Protein phosphatases play a key role in the modulation of synaptic activity by dephosphorylation of many signaling components involved in synaptic plasticity (Winder and Sweatt, 2001). Because the concentrations of Ng in the neuronal soma and dendritic spines are very high, a high level of PO_4-Ng could potentially serve as a competitive substrate for all those phosphatases and retard the dephosphorylation of other signaling phosphoproteins, thereby further enhancing synaptic response.

Ng has been implicated in neuronal signaling to modulate synaptic plasticity and cognitive behaviors (Gerendasy and Sutcliffe, 1997; Pak et al., 2000; Miyakawa et al., 2001). However, the electrophysiological phenotype reported here using our $Ng^{-/-}$ mice is different from that reported recently by Krucker et al. (2002). In contrast to the observed attenuation of LTP in our $Ng^{-/-}$ mice, the other Ng mutant strain (Krucker et al., 2002) displayed enhanced LTP over the wild type at 100 Hz. Even low-frequency stimulations at 1 and 5 Hz for 900 pulses, which normally induce moderate LTD in the adult wild-type mice, generated a high level of potentiation in those mutant mice. Our current results clearly demonstrate that $Ng^{-/-}$ mice are deficient in the HFS (100 Hz)-induced LTP and are able to express modest LTD by low-frequency (1 and 5 Hz) stimulations (Figs. 5, 6). Even at 10 Hz stimulation, our $Ng^{-/-}$ mice express low levels of LTD, whereas the wild-type mice exhibit moderate LTP. Detailed analysis of the synaptic responses during and after 10 Hz stimulation provides evidence that presynaptic functions (PPF and synaptic fatigue) of $Ng^{-/-}$ mice are similar to those of $Ng^{+/+}$ mice; however, the posttetanic responses (postsynaptic signaling and remodeling) are depressed in $Ng^{-/-}$ mice (Fig. 7). The different results obtained from the two independently generated Ng mutant strains may be attributable to the expression of two distinct gene products. In our $Ng^{-/-}$ mice (Pak et al., 2000), the entire Ng molecule was replaced by β-galactosidase, whereas in the mutant mice generated by Krucker et al. (2002), a fusion protein of the Ng N-terminal 30 amino acids and β-galactosidase was expressed. Although this N-terminal region does not contain the PKC phosphorylation site or the CaM-binding domain, it is fairly acidic (7 Asp and only 1 Lys) and rich in Cys (three residues), and its neuronal function is unknown. Interestingly, both strains of mice exhibit a lower level of the autophosphorylated CaMKII in the hippocampal slices. In addition, our $Ng^{-/-}$ mice exhibit an overall attenuation of the Ca^{2+}- and Ca^{2+}–CaM-mediated signaling, including activation of PKC, PKA, p42 and p44 ERK, and CREB (Wu et al., 2002, 2003).The depression of these signaling cascades may contribute to the observed deficits in several cognitive behavioral tasks of our $Ng^{-/-}$ mice (Pak et al., 2000; Miyakawa et al., 2001). These results are in line with the prevailing notion that elevated levels of $[Ca^{2+}]_i$ favor enhanced synaptic responses and improve the performance of cognitive behavior tasks.

Behavioral testing with the Morris water maze was used to establish the relationship between the level of hippocampal Ng in mice and their performances of cognitive behavioral tasks. Unlike the fear-conditioning paradigm, which measures responses after one training session, learning to navigate the water maze requires many training sessions. Thus, it is practical to compare the learning scores among individuals during training and the probe test. Although hippocampal Ng contents among $Ng^{+/+}$ and $Ng^{+/-}$ mice vary widely, we observed a significant relationship between learning performances and Ng levels mainly among $Ng^{+/-}$ mice. On average, the Ng level in $Ng^{+/+}$ mice is approximately twice as much as that of $Ng^{+/-}$ mice; perhaps $Ng^{+/+}$ mice already reach the ceiling effect for normal performance of these tasks. After extensive training, both $Ng^{+/+}$ and $Ng^{+/-}$ mice, but not $Ng^{-/-}$ mice, reach the training criterion in the hidden-platform trial, indicating that even a low level of Ng can enhance learning to locate the hidden platform. Likewise, a sig-

nificant relationship between the level of Ng and the performances of $Ng^{+/-}$ mice was also seen in the probe test. Surprisingly, the performances of the low-Ng group of $Ng^{+/-}$ mice were as low as those of $Ng^{-/-}$ mice, suggesting that low levels of hippocampal Ng have an insignificant effect on the performance of the probe test. A parsimonious explanation for this observation is that the probe test has a greater demand for Ng (a higher threshold) than acquisition of the task during the hidden-platform trial.

The hippocampal level of Ng has been shown to decline significantly in aging mice (Enderlin et al., 1997; Mons et al., 2001), and their reduction in Ng could contribute to the decline in cognitive functions among an aging population. The high variance of hippocampal Ng levels in mice could reflect the genetic variability of the population and variable responses to environmental stimuli as well as differences in ages and rates of protein turnover. It is also possible that training of the mice during behavioral testing affects their hippocampal Ng levels and the degree of Ng phosphorylation. For example, an increase in PKCγ activity after training has been shown (Van der Zee et al., 1992), and this could lead to an increase in Ng phosphorylation as well as its expression based on our previous *in vitro* assay showing the stimulation of rat Ng promoter–reporter activity by PKC (Sato et al., 1995). Furthermore, it has been reported that thyroid hormone (Iniguez et al., 1992, 1996; Etchamendy et al., 2001, 2003) and retinoic acid (Etchamendy et al., 2001, 2003) enhanced the expression of this protein. Thus, Ng can be considered as a synaptic plasticity enhancer, and its expression may be regulated by hormones and by environmental factors. In this regard, it is interesting to note that the 3′-untranslated region (UTR) of Ng mRNA contains dendritic targeting sequences (Mori et al., 2000) and its 5′-UTR contains an internal ribosomal entry site for efficient translation of Ng in dendrites (Pinkstaff et al., 2001). All of these observations point to a possible activity-dependent local synthesis of Ng to enhance synaptic plasticity.

References

Bernal J, Rodriguez-Pena A, Iniguez MA, Ibarrola N, Munoz A (1992) Influence of thyroid hormone on brain gene expression. Acta Med Austriaca 19 [Suppl 1]:32–35.

Bhalla US, Iyengar R (1999) Emergent properties of networks of biological signaling pathways. Science 283:381–387.

Chakravarthy B, Morley P, Whitfield J (1999) Ca^{2+}-calmodulin and protein kinase Cs: a hypothetical synthesis of their conflicting convergences on shared substrate domains. Trends Neurosci 22:12–16.

Cimler BM, Andreasen TJ, Andreasen KI, Storm DR (1985) P-57 is a neural specific calmodulin-binding protein. J Biol Chem 260:10784–10788.

Cohen RW, Margulies JE, Coulter II PM, Watson JB (1993) Functional consequences of expression of the neuron-specific, protein kinase C substrate RC3 (neurogranin) in *Xenopus* oocytes. Brain Res 627:147–152.

Derkach V, Barria A, Soderling TR (1999) Ca^{2+}/calmodulin-kinase II enhances channel conductance of alpha-amino-3-hydroxy-5-methyl-4-isoxazolepropionate type glutamate receptors. Proc Natl Acad Sci USA 96:3269–3274.

Enderlin V, Pallet V, Alfos S, Dargelos E, Jaffard R, Garcin H, Higueret P (1997) Age-related decreases in mRNA for brain nuclear receptors and target genes are reversed by retinoic acid treatment. Neurosci Lett 229:125–129.

Erondu NE, Kennedy MB (1985) Regional distribution of type II Ca^{2+}/calmodulin-dependent protein kinase in rat brain. J Neurosci 5:3270–3277.

Etchamendy N, Enderlin V, Marighetto A, Vouimba RM, Pallet V, Jaffard R, Higueret P (2001) Alleviation of a selective age-related relational memory deficit in mice by pharmacologically induced normalization of brain retinoid signaling. J Neurosci 21:6423–6429.

Etchamendy N, Enderlin V, Marighetto A, Pallet V, Higueret P, Jaffard R (2003) Vitamin A deficiency and relational memory deficit in adult mice: relationships with changes in brain retinoid signalling. Behav Brain Res 145:37–49.

Gerendasy DD, Sutcliffe JG (1997) RC3/neurogranin, a postsynaptic calpacitin for setting the response threshold to calcium influxes. Mol Neurobiol 15:131–163.

Giese KP, Fedorov NB, Filipkowski RK, Silva AJ (1998) Autophosphorylation at Thr286 of the alpha calcium-calmodulin kinase II in LTP and learning. Science 279:870–873.

Huang KP, Huang FL (2002) Glutathionylation of proteins by glutathione disulfide S-oxide. Biochem Pharmacol 64:1049–1056.

Huang KP, Huang FL, Chen HC (1993) Characterization of a 7.5-kDa protein kinase C substrate (RC3 protein, neurogranin) from rat brain. Arch Biochem Biophys 305:570–580.

Huang KP, Huang FL, Li J, Schuck P, McPhie P (2000) Calcium-sensitive interaction between calmodulin and modified forms of rat brain neurogranin/RC3. Biochemistry 39:7291–7299.

Husson M, Enderlin V, Alfos S, Feart C, Higueret P, Pallet V (2003) Triiodothyronine administration reverses vitamin A deficiency-related hypoexpression of retinoic acid and triiodothyronine nuclear receptors and of neurogranin in rat brain. Br J Nutr 90:191–198.

Impey S, Obrietan K, Storm DR (1999) Making new connections: role of ERK/MAP kinase signaling in neuronal plasticity. Neuron 23:11–14.

Iniguez MA, Rodriguez-Pena A, Ibarrola N, Morreale de Escobar G, Bernal J (1992) Adult rat brain is sensitive to thyroid hormone. Regulation of RC3/neurogranin mRNA. J Clin Invest 90:554–558.

Iniguez MA, De Lecea L, Guadano-Ferraz A, Morte B, Gerendasy D, Sutcliffe JG, Bernal J (1996) Cell-specific effects of thyroid hormone on RC3/neurogranin expression in rat brain. Endocrinology 137:1032–1041.

Krucker T, Siggins GR, McNamara RK, Lindsley KA, Dao A, Allison DW, De Lecea L, Lovenberg TW, Sutcliffe JG, Gerendasy DD (2002) Targeted disruption of RC3 reveals a calmodulin-based mechanism for regulating metaplasticity in the hippocampus. J Neurosci 22:5525–5535.

Leonard AS, Bayer KU, Merrill MA, Lim IA, Shea MA, Schulman H, Hell JW (2002) Regulation of calcium/calmodulin-dependent protein kinase II docking to *N*-methyl-D-aspartate receptors by calcium/calmodulin and alpha-actinin. J Biol Chem 277:48441–48448.

Li J, Pak JH, Huang FL, Huang KP (1999) *N*-methyl-D-aspartate induces neurogranin/RC3 oxidation in rat brain slices. J Biol Chem 274:1294–1300.

Li J, Huang FL, Huang KP (2001) Glutathiolation of proteins by glutathione disulfide S-oxide derived from S-nitrosoglutathione. Modifications of rat brain neurogranin/RC3 and neuromodulin/GAP-43. J Biol Chem 276:3098–3105.

Lisman J, Schulman H, Cline H (2002) The molecular basis of CaMKII function in synaptic and behavioural memory. Nat Rev Neurosci 3:175–190.

Lisman JE (2001) Three Ca^{2+} levels affect plasticity differently: the LTP zone, the LTD zone and no man's land. J Physiol (Lond) 532:285.

Lisman JE, Zhabotinsky AM (2001) A model of synaptic memory: a CaMKII/PP1 switch that potentiates transmission by organizing an AMPA receptor anchoring assembly. Neuron 31:191–201.

Mahoney CW, Pak JH, Huang KP (1996) Nitric oxide modification of rat brain neurogranin. Identification of the cysteine residues involved in intramolecular disulfide bridge formation using site-directed mutagenesis. J Biol Chem 271:28798–28804.

Miyakawa T, Yared E, Pak JH, Huang FL, Huang KP, Crawley JN (2001) Neurogranin null mutant mice display performance deficits on spatial learning tasks with anxiety related components. Hippocampus 11:763–775.

Mons N, Enderlin V, Jaffard R, Higueret P (2001) Selective age-related changes in the PKC-sensitive, calmodulin-binding protein, neurogranin, in the mouse brain. J Neurochem 79:859–867.

Mori Y, Imaizumi K, Katayama T, Yoneda T, Tohyama M (2000) Two cis-acting elements in the 3′ untranslated region of alpha-CaMKII regulate its dendritic targeting. Nat Neurosci 3:1079–1084.

Pak JH, Huang FL, Li J, Balschun D, Reymann KG, Chiang C, Westphal H, Huang KP (2000) Involvement of neurogranin in the modulation of calcium/calmodulin-dependent protein kinase II, synaptic plasticity, and spatial learning: a study with knockout mice. Proc Natl Acad Sci USA 97:11232–11237.

Paulsen O, Sejnowski TJ (2000) Natural patterns of activity and long-term synaptic plasticity. Curr Opin Neurobiol 10:172–179.

Pinkstaff JK, Chappell SA, Mauro VP, Edelman GM, Krushel LA (2001) Internal initiation of translation of five dendritically localized neuronal mRNAs. Proc Natl Acad Sci USA 98:2770–2775.

Prast H, Philippu A (2001) Nitric oxide as modulator of neuronal function. Prog Neurobiol 64:51–68.

Sato T, Xiao DM, Li H, Huang FL, Huang KP (1995) Structure and regulation of the gene encoding the neuron-specific protein kinase C substrate neurogranin (RC3 protein). J Biol Chem 270:10314–10322.

Seki K, Chen HC, Huang KP (1995) Dephosphorylation of protein kinase C substrates, neurogranin, neuromodulin, and MARCKS, by calcineurin and protein phosphatases 1 and 2A. Arch Biochem Biophys 316:673–679.

Sheu FS, Mahoney CW, Seki K, Huang KP (1996) Nitric oxide modification of rat brain neurogranin affects its phosphorylation by protein kinase C and affinity for calmodulin. J Biol Chem 271:22407–22413.

Silva AJ, Wang Y, Paylor R, Wehner JM, Stevens CF, Tonegawa S (1992) Alpha calcium/calmodulin kinase II mutant mice: deficient long-term potentiation and impaired spatial learning. Cold Spring Harb Symp Quant Biol 57:527–539.

Strack S, Colbran RJ (1998) Autophosphorylation-dependent targeting of calcium/ calmodulin-dependent protein kinase II by the NR2B subunit of the *N*-methyl-D-aspartate receptor. J Biol Chem 273:20689–20692.

Tallant EA, Cheung WY (1983) Calmodulin-dependent protein phosphatase: a developmental study. Biochemistry 22:3630–3635.

Tang WJ, Hurley JH (1998) Catalytic mechanism and regulation of mammalian adenylyl cyclases. Mol Pharmacol 54:231–240.

Van der Zee EA, Compaan JC, de Boer M, Luiten PG (1992) Changes in PKC γ immunoreactivity in mouse hippocampus induced by spatial discrimination learning. J Neurosci 12:4808–4815.

Wexler EM, Stanton PK, Nawy S (1998) Nitric oxide depresses $GABA_A$ receptor function via coactivation of cGMP-dependent kinase and phosphodiesterase. J Neurosci 18:2342–2349.

Wilsch VW, Behnisch T, Jager T, Reymann KG, Balschun D (1998) When are class I metabotropic glutamate receptors necessary for long-term potentiation? J Neurosci 18:6071–6080.

Winder DG, Sweatt JD (2001) Roles of serine/threonine phosphatases in hippocampal synaptic plasticity. Nat Rev Neurosci 2:461–474.

Wong ST, Athos J, Figueroa XA, Pineda VV, Schaefer ML, Chavkin CC, Muglia LJ, Storm DR (1999) Calcium-stimulated adenylyl cyclase activity is critical for hippocampus-dependent long-term memory and late phase LTP. Neuron 23:787–798.

Wu J, Li J, Huang KP, Huang FL (2002) Attenuation of protein kinase C and cAMP-dependent protein kinase signal transduction in the neurogranin knockout mouse. J Biol Chem 277:19498–19505.

Wu J, Huang KP, Huang FL (2003) Participation of NMDA-mediated phosphorylation and oxidation of neurogranin in the regulation of Ca^{2+}- and Ca^{2+}/calmodulin-dependent neuronal signaling in the hippocampus. J Neurochem 86:1524–1533.

Zarri I, Bucossi G, Cupello A, Rapallino MV, Robello M (1994) Modulation by nitric oxide of rat brain GABAA receptors. Neurosci Lett 180:239–242.

Zheng X, Zhang L, Wang AP, Bennett MV, Zukin RS (1999) Protein kinase C potentiation of *N*-methyl-D-aspartate receptor activity is not mediated by phosphorylation of *N*-methyl-D-aspartate receptor subunits. Proc Natl Acad Sci USA 96:15262–15267.